

Supporting Information

3D-printed microneedle-extraction system integrated with patterned electrodes for minimally invasive transdermal detection

- Supporting Information

Changyuan Zhan¹⁺, Fanmao Liu²⁺, Zhiran Shen¹, Xinshuo Huang¹, Shuang Huang¹, Xiangling Li¹,
Jing Liu,² Jiang Yang,³ Jiefeng Xu,⁴ Xi Xie^{1,*} and Hui-Juan Chen^{1,*}

¹State Key Laboratory of Optoelectronic Materials and Technologies, Guangdong Province Key
Laboratory of Display Material and Technology, School of Electronics and Information Technology,
Sun Yat-Sen University, Guangzhou, China

²The First Affiliated Hospital of Sun Yat-sen University, Guangzhou, China

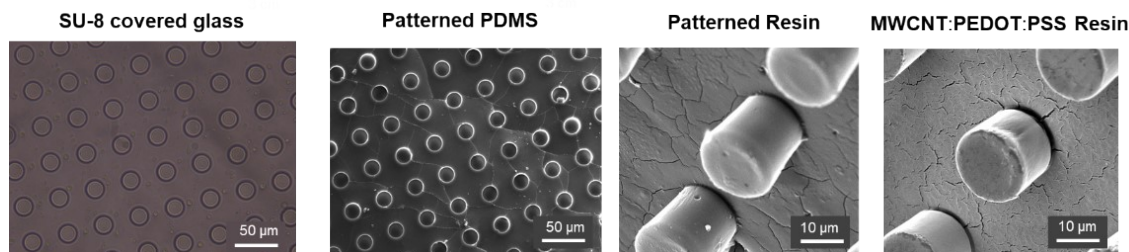
³State Key Laboratory of Oncology in South China, Sun Yat-sen University Cancer Center,
Guangzhou, China

⁴Key Laboratory of The Diagnosis and Treatment of Severe Trauma and Burn of Zhejiang Province,
The Second Affiliated Hospital of Zhejiang University School of Medicine, Hangzhou, China

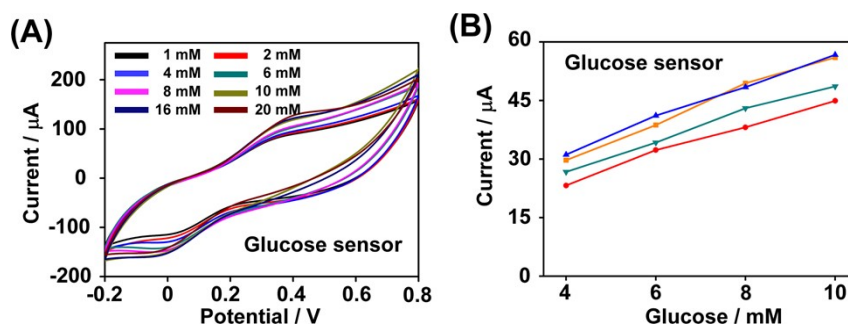
CORRESPONDING AUTHOR FOOTNOTE:

Email: Hui-Juan Chen, chenhuix5@mail.sysu.edu.cn; Xi Xie, xiexi27@mail.sysu.edu.cn

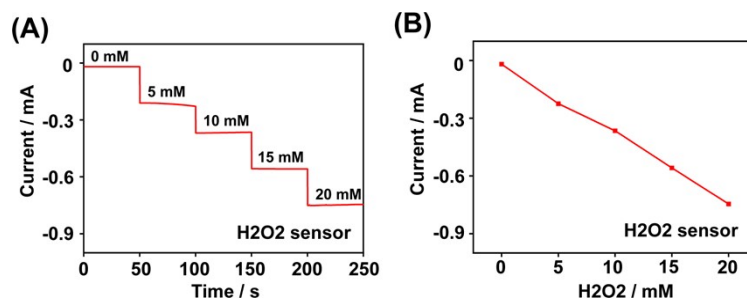
⁺ These authors contributed equally to this work.



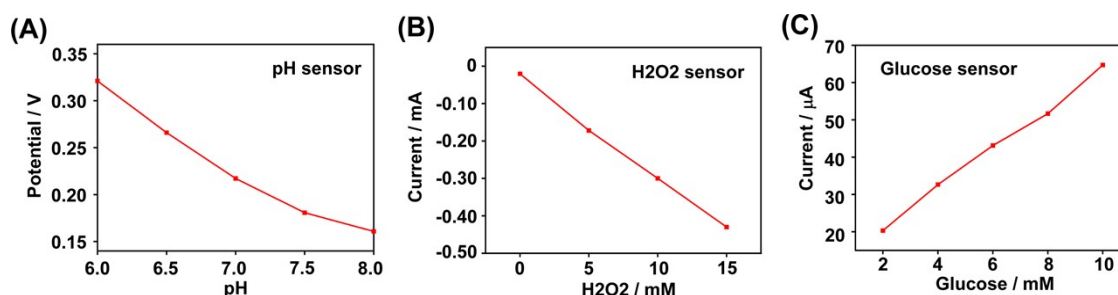
Extended Data Figure 1 | Optical images and SEM images of patterned PDMS and resin.



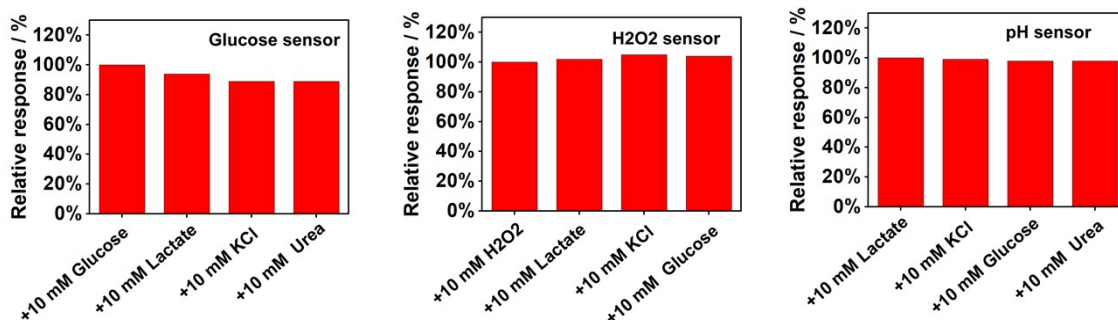
Extended Data Figure 2 | (A) Cyclic voltammetry of glucose sensor coated with MWCNT: PEDOT: PSS in $K_3[Fe(CN)_6]$ solutions with different concentrations. (B) Reproducibility experiment for glucose sensors (n=4).



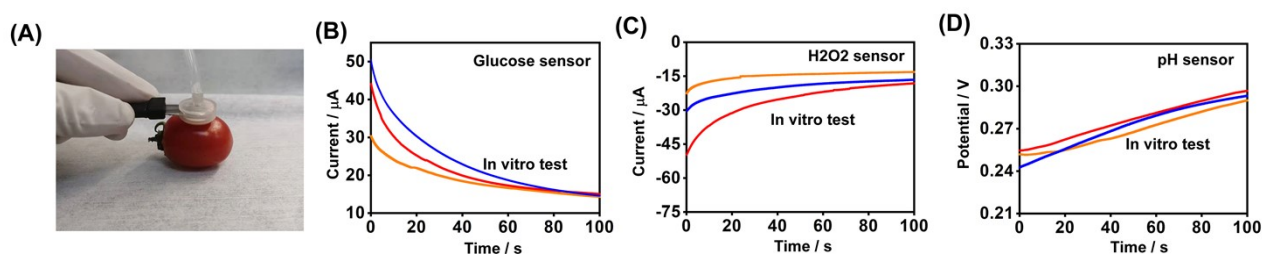
Extended Data Figure 3 | H₂O₂ biosensor performance in presence of different concentrations of H₂O₂. (A) Step response of H₂O₂ biosensor in 0 to 20 mM H₂O₂; (B) Corresponding calibration plot of responding current vs H₂O₂ concentration.



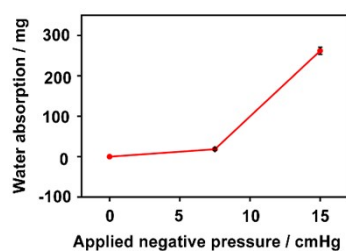
Extended Data Figure 4 | Biosensor performance in conjunction with prepared three-electrode system or two-electrode system. Calibration curve of potential response of (A) pH sensor. Calibration curve of amperometric response of (B) H₂O₂ sensor and (C) glucose sensor.



Extended Data Figure 5 | Relative signals of (A) glucose, (B) H₂O₂, (C) pH sensors with the addition of interfering substances. The recorded signal of the corresponding marker for each sensor was set to 100% for comparison.



Extended Data Figure 6 | Skin-penetrating and sensing performance verification on the cherry tomato. (A) Cherry tomato with an applied MN arrays device. Reproducibility experiment of (B) glucose sensor, (C) H₂O₂ sensor, and (D) pH sensor on the cherry tomato model (n=3). Data were recorded at 5-min intervals.



Extended Data Figure 7 | Evaluation of water absorption at negative pressure of 0, 7.5, and 15 cmHg by MN extraction.